Transient and stationary chaos of a Bose-Einstein condensate loaded into a moving optical lattice potential

Guishu Chong, Wenhua Hai,* and Qiongtao Xie
Department of Physics, Hunan Normal University, Changsha 410081, People's Republic of China
(Received 9 March 2004; published 27 September 2004)

Chaotic space-time evolution is investigated for the particle number density of a Bose-Einstein condensate with attractive interatomic interaction loaded into a traveling optical lattice. Melnikov chaos is studied and the weakly chaotic regime is presented analytically. Transitions from transient to stationary chaos in the space-time evolution are illustrated numerically. The results show that, on increasing the strength of the optical potential, the transient chaos falls onto several different attractors. Meanwhile, these attractors undergo a series of period-doubling bifurcations when the optical potential intensity is increased continuously, and eventually stationary chaos arises for a critical depth of the optical lattice. The obstructions to chaos caused by the damping and the motion of lattice are also demonstrated.

DOI: 10.1103/PhysRevE.70.036213 PACS number(s): 05.45.Ac, 03.75.Lm, 03.75.Kk, 39.25.+k

I. INTRODUCTION

Periodic optical lattices, formed by the interference of two or more laser beams, have been extensively used in atomic physics [1–3]. The combination of the optical lattices with a Bose-Einstein condensate (BEC) in recent experiments opened up many new research aspects [4–12] and provided a practically useful method to precisely manipulate BECs [13]. Correlated subjects include the observation of quantum phase effects [4,14], superfluidity [15,16], atomic number squeezing [9,17], matter-wave transport [8], quantum computation and quantum information [18,19], detection of periodic structure [20], phase transitions from superfluids to Mott insulators [5,21,22], and so on. By using a periodic laser standing wave, an array of Josephson junctions is created with the condensates trapped in the valleys of the periodic potential [12]. In the tight binding approximation (i.e., the many-mode approximation) or two-mode approximation (a simpler case of the former) [23], many characteristics, for instance, Josephson oscillating atomic currents [12] and chaos [24–27], are revealed. In addition to extensive investigations in static lattices, moving optical lattices have also been studied recently. For example, Ruprecht *et al.* [28] and Ohberg and Stenholm [29] early applied a traveling lattice to drive the BEC system. Denschlag *et al.* loaded the BEC into a traveling lattice to study the physical properties in a recent experiment [30]. Fallani *et al.* reported the lensing effect on a BEC expanding in a moving one-dimensional (1D) optical lattice, i.e., the optical lattice acts as a lens for the matter wave, focusing or defocusing the atomic cloud along the direction of the lattice [31].

It is well known that in the process of BEC collapse [32,33], chaos will emerge. Chaos may play a destructive role for the system. Therefore, predicting and controlling chaos are quite important in the formation and applications of BECs. For the system considered, chaos has also attracted extensive interest. In many previous works [24–27], the chaotic features in this system have been studied in the framework of the many-mode approximation [12] (characterization of the lattice system), or its simplified form, the two-mode approximation (description of a double-well or two-state system) [23]. In this scheme, integration over the spatial coordinates is performed, so only the time evolutional properties are presented, and the spatial behaviors of the system are unclear. In order to research the space-time chaos in such a system, we shall start the investigation from the time-dependent Gross-Pitaevskii (GP) equation, which governs the dynamics of the BEC system in mean-field theory [34]. We consider a damped BEC loaded into a traveling optical lattice. Under a deterministic perturbation, Melnikov chaos [35] in the space-time evolution of the BEC is investigated analytically for the case of an attractive atom-atom interaction. A homoclinic chaotic regime is obtained and the suppression effects of the damping and the propagation of the optical lattice on the onset of chaos are discussed. The transient chaos due to the dissipative role of the damping [24,36–38] is simulated numerically. For different intensities of the optical potential, the evolutional trajectories of the atomic number density fall onto different regular attractors after the transient chaos. These final attractors undergo a series of period-doubling bifurcations with increase of the optical intensity. When the optical intensity reaches a threshold value, regularity of the attractor is destroyed and the transient chaos changes to stationary chaos.

II. ANALYSIS OF THE CHAOTIC DYNAMICS

The BEC system considered here is created in a harmonically trapped potential and then is loaded into a moving optical lattice. The 3D combined potential therefore is given by $V(x,y,z,t)=V_0\cos^2(k\xi)+m(\omega_x^2x^2+\omega_y^2y^2+\omega_z^2z^2)/2$, where the second term is the harmonically magnetic potential with m being the atomic mass and $\omega_x,\omega_y,\omega_z$ the trap frequencies. The periodic potential is a moving optical lattice [30] with the space-time variable $\xi=x+\delta t/2k$, where δ is the frequency difference between the two counterpropagating laser

*Corresponding author.
Electronic address: adcve@public.cs.hn.cn

beams and k the laser wave vector which fixes the velocity of the traveling lattice as $v_L=\delta/(2k)$. When the BEC is formed in the region near the center of the magnetic trap, the magnetic potential is much weaker than the lattice one and can be neglected. According to the experimental parameters of Ref. [30], $\omega_x=\sqrt{2}\omega_y=2\omega_z=2\pi\times 27$ Hz, $k=2\pi/\lambda$, $\lambda=589$ nm, and m the mass of ^{23}Na, we find that in the region of $k\sqrt{x^2+y^2/2+z^2/4}\leqslant 100\pi$ the harmonic potential is of the order of $10^{-2}\,E_r$, which is much less than the lattice potential $V_0=14E_r$, where $E_r=\hbar^2k^2/(2m)$ is the recoil energy. Therefore, the 1D optical potential plays the main role for the system and the quasi-1D approximation is valid in this region. On the other hand, for a time-dependent lattice, the damping effect should be considered. The damping effect caused by the incoherent exchange of normal atoms and the finite temperature effect [39–41] has been analyzed in detail for the two-junction linking of two BECs [39]. For the system considered here, it is similar to the case of the linear junction linking of many BECs. Thus, a damping effect caused by similar elements or other factors may also exist. With these considerations, the system is governed by the following quasi-1D GP equation [42]:

$$i\hbar(1-i\gamma)\frac{\partial\psi}{\partial t}=-\frac{\hbar^2}{2m}\frac{\partial^2\psi}{\partial x^2}+g_0|\psi|^2\psi+V_0\cos^2(k\xi)\psi, \quad (1)$$

where ψ is the macroscopic quantum wave function, $g_0=4\pi\hbar^2a/m$ characterizes the interatomic interaction strength with a being the s-wave scattering length, $a>0$ denotes a repulsive interaction and $a<0$ corresponds to an attractive interaction, and the term proportional to γ represents the damping effect which was used in Ref. [42].

Due to the complexity of Eq. (1), we focus our interest on only the traveling wave solution of this equation and write it in the form

$$\psi=\varphi(\xi)\exp[i(\alpha x+\beta t)], \quad (2)$$

such that the matter wave is a Bloch-like wave. Here, α and β are two undetermined real constants. According to the definition of the space-time variable $\xi=x+v_Lt$ in the former, the traveling wave $\varphi(\xi)$ moves with the same velocity as the optical lattice. Inserting Eq. (2) into Eq. (1), we can easily turn the partial differential equation (1) into an ordinary differential one:

$$\frac{\hbar^2}{2m}\frac{d^2\varphi}{d\xi^2}+i\left(\frac{\hbar^2\alpha}{m}+\hbar v_L-i\hbar\gamma v_L\right)\frac{d\varphi}{d\xi}-\left(\hbar\beta+\frac{\hbar^2\alpha^2}{2m}-i\hbar\beta\gamma\right)\varphi-g_0|\varphi|^2\varphi=V_0\cos^2(k\xi)\varphi. \quad (3)$$

For simplicity, using the dimensionless variables and parameters

$$\zeta=k\xi,\quad v=2mv_L/\hbar k,\quad \tilde{\beta}=\hbar\beta/E_r,$$

$$\tilde{\alpha}=\alpha/k,\quad \tilde{V}_0=V_0/E_r, \quad (4)$$

we have Eq. (3) in the form

$$\frac{d^2\varphi}{d\zeta^2}+i(v+2\tilde{\alpha})\frac{d\varphi}{d\zeta}+\gamma v\frac{d\varphi}{d\zeta}-(\tilde{\beta}+\tilde{\alpha}^2)\varphi+i\gamma\tilde{\beta}\varphi-g|\varphi|^2\varphi=\tilde{V}_0\cos^2(\zeta)\varphi \quad (5)$$

with the dimensionless strength $g=8\pi ak$ and the function φ being normalized by $k^{1/2}$. Writing the complex function φ in the form of $\varphi=R(\zeta)e^{i\theta(\zeta)}$ and entering it in the above equation, we obtain two coupled equations between the real functions R and θ as

$$\frac{d^2R}{d\zeta^2}-R\left(\frac{d\theta}{d\zeta}\right)^2-(v+2\tilde{\alpha})R\frac{d\theta}{d\zeta}+\gamma v\frac{dR}{d\zeta}-(\tilde{\beta}+\tilde{\alpha}^2)R-gR^3=\tilde{V}_0\cos^2(\zeta)R, \quad (6)$$

$$2\frac{dR}{d\zeta}\frac{d\theta}{d\zeta}+R\frac{d^2\theta}{d\zeta^2}+(v+2\tilde{\alpha})\frac{dR}{d\zeta}+\gamma vR\frac{d\theta}{d\zeta}+\gamma\tilde{\beta}R=0. \quad (7)$$

Clearly, the square of the amplitude R is just the particle number density because $|R|=|\varphi|=|\psi|$, and θ is the phase of φ. It is not difficult to observe that when the phase has a linear relation with the space-time variable, i.e., $d\theta/d\zeta=-\tilde{\beta}/v=-(v/2+\tilde{\alpha})$, Eq. (7) can be naturally satisfied. Consequently, Eq. (6) is changed to

$$\frac{d^2R}{d\zeta^2}-\frac{1}{4}v^2R-gR^3=\tilde{V}_0\cos^2(\zeta)R-\gamma v\frac{dR}{d\zeta}. \quad (8)$$

Obviously, the particularly linear relation between θ and ζ taken here leads to the coefficient of the R term on the left hand side of Eq. (8) having a fixed negative sign. According to the general theory of the Duffing equation, underlying Eq. (10) has a homoclinic solution only when the coefficients of the linear (R) and nonlinear (R^3) terms on the left hand side of Eq. (8) have opposite signs [43]. Therefore, in order to study the homoclinic chaos for the negative R term we must consider the case of attractive atom-atom interactions, i.e., $g<0$; then the above equation is just the parametrically driven Duffing equation with a damping term [43,44]. The chaotic features of the Duffing system have been extensively researched [45,46]. If the phase θ does not take a special linear relation with ζ, the dynamical behaviors of the system can be investigated from the coupled equations (6) and (7) directly both for repulsive and attractive condensates, and the chaotic behavior becomes more complex; this will not be discussed here.

For the case of a weak optical lattice potential and damping, a perturbational treatment is permitted. It is well known that the Melnikov-function method [35,44] is a valid analytical one under the first order approximation. Making the perturbational expansion

$$R(\zeta)=R_0(\zeta)+R_1(\zeta),\ |R_1|\ll|R_0|, \quad (9)$$

and inserting it into Eq. (8), we obtain the leading and first order equations as

$$\frac{d^2R_0}{d\zeta^2}-\frac{1}{4}v^2R_0-gR_0^3=0, \quad (10)$$

$$\frac{d^2R_1(\zeta)}{d\zeta} - \frac{1}{4}v^2R_1(\zeta) - 3gR_0^2(\zeta)R_1(\zeta)$$

$$= \tilde{V}_0\cos^2(\zeta)R_1(\zeta) - \gamma v\frac{dR_1(\zeta)}{d\zeta}. \tag{11}$$

Starting from Eq. (10), the leading order equation has the homoclinic solution

$$R_0(\zeta) = \frac{v}{\sqrt{-2g}}\mathrm{sech}\left(\frac{v}{2}(\zeta+\zeta_0)\right), \tag{12}$$

where ζ_0 is an integration constant. Obviously, under weak perturbations the leading order solution of the number density is just a bright soliton solution, which implies that the wave packet of the matter wave is localized in the space at any time. Therefore, following the standard Melnikov approach, the Melnikov function for this homoclinic orbit is given by

$$M_{\pm}(\zeta_0) = \int_{-\infty}^{\infty}\frac{dR_0}{d\zeta}\left(\tilde{V}_0\cos^2(\zeta)R_0 - \gamma v\frac{dR_0}{d\zeta}\right)d\zeta$$

$$= -\frac{\gamma v^4}{6g} - \frac{2\pi\tilde{V}_0}{g}\mathrm{csch}\left(\frac{2\pi}{v}\right)\sin(2\zeta_0), \tag{13}$$

which measures the distance between the stable and unstable manifolds in the Poincaré section. If it has a simple zero, then a homoclinic bifurcation occurs, which signifies the onset of Smale-horseshoe chaotic behavior [44]. Taking note of Eq. (4), the Melnikov function (13) vanishing leads to the homoclinic chaotic region

$$\frac{V_0}{E_{r,0}} \geqslant \frac{16\gamma m^4 v_L^4}{3\pi\hbar^4k_0^2k^2}\sinh\left(\frac{\pi\hbar k}{mv_L}\right), \tag{14}$$

in which Eq. (4) has been adopted. In Eq. (14), we express the optical intensity as a function of the wave vector k and the moving velocity v_L of the optical lattice. Since k is involved in the recoil energy E_r, which is used as the unit of optical strength in the definition of Eq. (4), in order to see clearly the dependence of the optical intensity on the wave vector k, we introduce another energy scale of $E_{r,0}=\hbar^2k_0^2/(2m)$ for a fixed optical wavelength $\lambda_0=2\pi/k_0=589$ nm just as in Eq. (14). The criterion (14) is usually considered as a necessary condition for the onset of chaos. For a set of fixed parameters Eq. (14) gives the threshold value of the optical potential. The system undergoes a procession from regular motion to chaotic motion when the strength of the optical potential is increased across the threshold value.

In order to see clearly the dependence of the chaotic regions on the system parameters, starting from Eq. (14), we plot the optical intensity V_0 versus the laser wave vector k in Fig. 1(a) and plot V_0 versus the traveling velocity v_L in Fig. 1(b). Here, the parameters are taken as $\gamma=0.005$, $m=23m_p$ with m_p the proton mass, and $\lambda_0=589$ nm; meanwhile, in Fig. 1(a) $v_L=3$ cm/s and V_0 and k are in units of $E_{r,0}$ and $k_0=2\pi/\lambda_0$, respectively, and in Fig. 1(b) $k=k_0$, V_0 and v_L are in units of $E_{r,0}$ and $v_{L,0}=3$ cm/s (a particular velocity scale selected arbitrarily). In Fig. 1, the areas above the curves

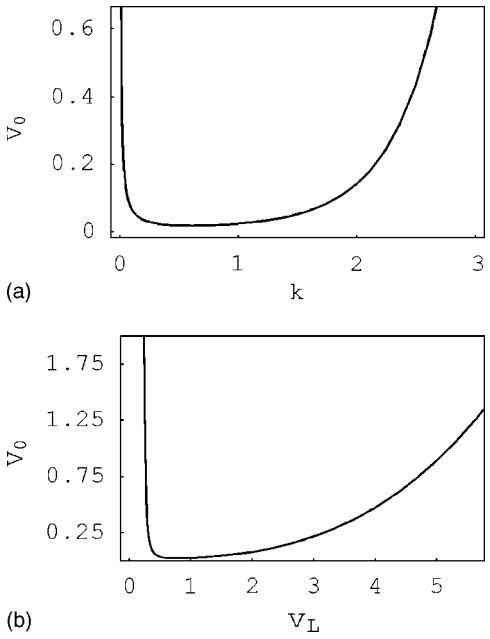

FIG. 1. Plots of the chaotic regions in parameter space of (a) the optical intensity V_0 versus the laser wave vector k and (b) V_0 versus the propagating velocity of the optical lattice from Eq. (14). Here the other system parameters are taken as $\gamma=0.005, m=23m_p, k_0=2\pi/\lambda_0=2\pi/589$ nm, $v_{L,0}=3$ cm/s, and V_0, k, v_L are in units of $E_{r,0}, k_0, v_{L,0}$, respectively.

correspond to Melnikov chaotic regions in which the evolution of the atomic number density has the properties of Smale-horseshoe chaos; those below denote regions of regular motion. From Fig. 1(a) we observe that for very weak damping $\gamma=0.005$, the threshold value of the laser intensity is approximately obtained as $V_0=0.02$ for $k=0.5$ (in unit of k_0). This implies that for weak damping and optical lattice potential the criterion (14) can indeed be satisfied. If the damping is increased to about 0.1, from Eq. (14), the critical value becomes $V_0=0.4$ for $k=0.5$. In this case, the optical strength becomes comparable to the interatomic interaction due to $g=8\pi ka=-0.375$ with s-wave scattering length $a=-2.8$ nm. Therefore, the optical potential cannot be treated as a perturbation now. On the other hand, from Fig. 1(b) we find that after $v_L>1$ a larger v_L value is associated with a larger threshold value of V_0. This implies a suppression of chaos, namely, in the region $v_L>1$, a given V_0 value is greater than the chaos threshold for a smaller v_L value, but it is less than the chaos threshold when v_L is increased to a certain value. Due to the experimental controllability of the lattice velocity, this suppressive effect suggested to us a valid approach to controlling the chaos in experiments. Moreover, to guarantee the validity of the weakly chaotic region (14), the traveling velocity of the lattice must be slow, because when the velocity is large enough the second term on the right hand of Eq. (8) may become very large and so the perturbational treatment becomes invalid. Meanwhile, from Eq. (14) we can see that the threshold value is proportional to the strength of the damping; when the damping is very weak, the critical V_0 value is small, but a strong damping will lead to a higher critical V_0. In other words, for a certain

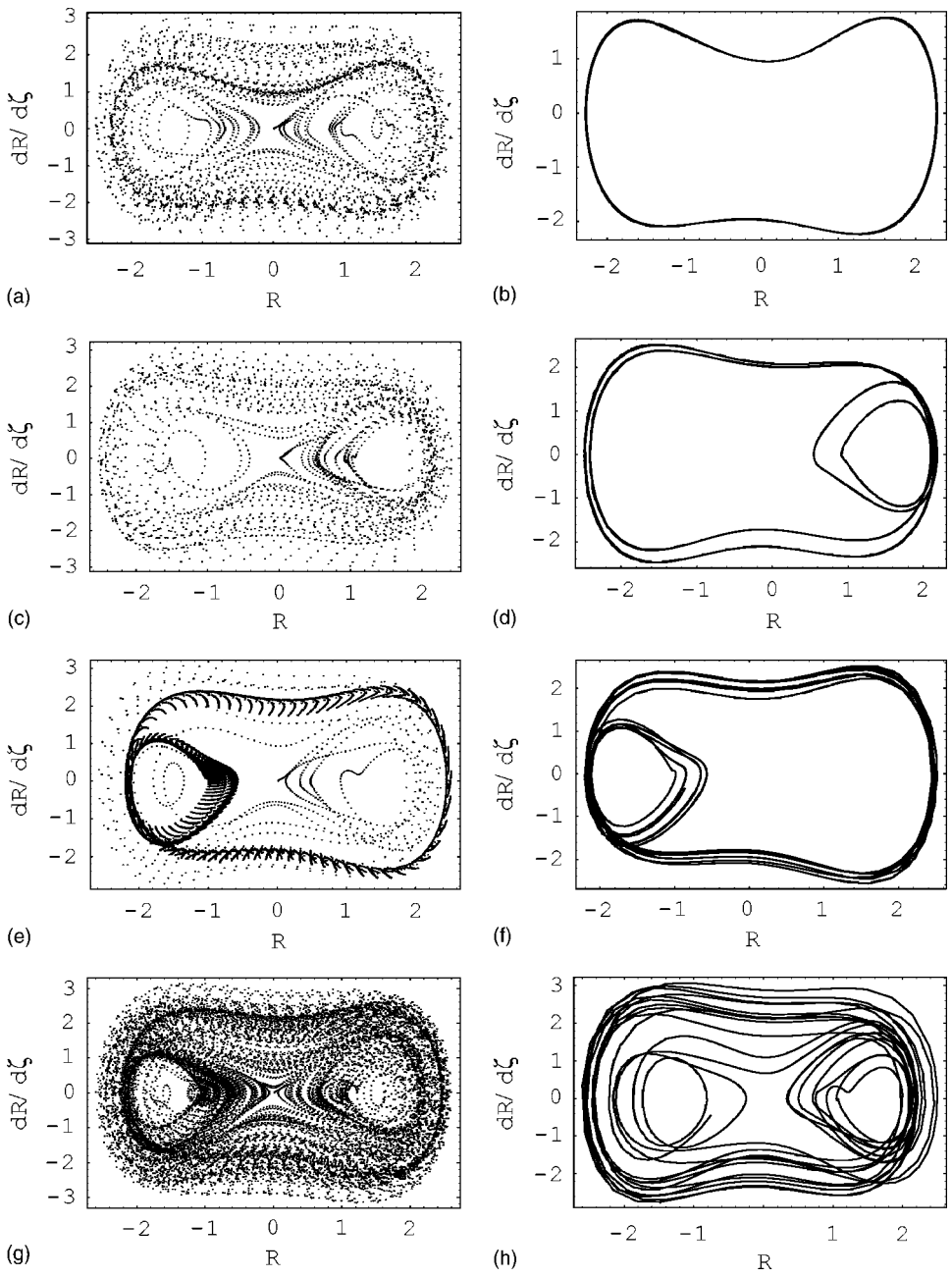

FIG. 2. Plots of the phase orbits in the equivalent phase space of $(R, dR/d\zeta)$ from Eq. (8). The left column shows the transient chaos and the right column illustrates the corresponding regular attractors and the stationary chaotic attractor (h).

depth of lattice, enhancement of the damping will decrease the chaotic region; so the damping has a suppressive effect on chaos too. However, when the damping is strong enough, the Melnikov method becomes invalid; then a numerical analysis for the system is needed.

III. NUMERICAL ILLUSTRATION OF THE TRANSITION FROM TRANSIENT TO STATIONARY CHAOS

Because of the damping effects, the dissipative system considered has the important consequence that the phase-space volume will contract with the evolution of the space-time variable. In the process of evolution, there exists the general feature that the evolution of the system seems to be chaotic during some transient periods and ultimately tends to some periodical stable attractors. This phenomenon is called transient chaos [36]. Transient chaos will appear for arbitrary initial conditions before it goes into the final attractors. We shall illustrate transient chaos in the numerical simulation by exhibiting the process of attraction from transient chaos to regular and stationary chaotic attractors.

We adopt Denschlag's experimental parameters, where m equates to $23m_p$ with m_p being the proton mass, the laser wavelength is $\lambda=\lambda_0=589$ nm, and the traveling velocity of the optical lattice reads $v_L=3$ cm/s such that $v=2mv_L/\hbar k_0=2.03$ and $g=8\pi k_0 a=-0.75$. Furthermore, a damping value

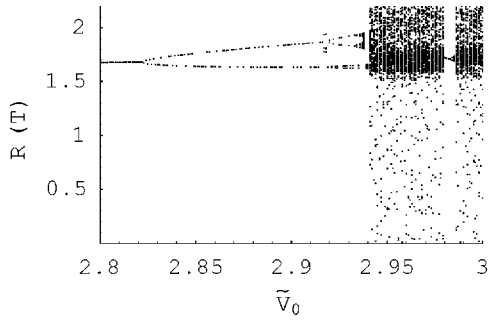

FIG. 3. A plot of the bifurcation diagram with $R(T)$ vs $\widetilde{V}_0$. At about $\widetilde{V}_0=2.95$, the system enters a stationary chaotic state. Here, $\widetilde{V}_0$ is in units of the recoil energy $E_{r,0}$.

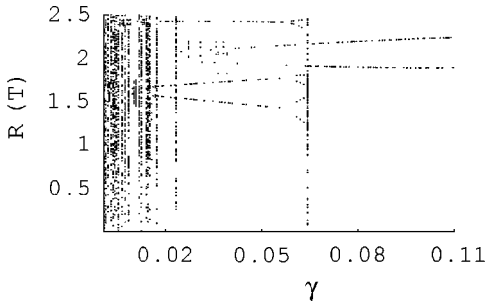

FIG. 4. A plot of the bifurcation diagram of $R(T)$ vs γ. The chaos suppression effect caused by damping is illustrated. With an increase of the damping, the system changes from chaotic to regular motion.

$\gamma=0.05$ is set. Using MATHEMATICA we solve Eq. (8) numerically under the initial conditions $R(0)=0.01$, $dR(0)/d\zeta=0$, and illustrate the transient and final attractors in the equivalent phase space of $(R, dR/d\zeta)$ by Fig. 2 for (a) and (b) with $\widetilde{V}_0=1.85$, (c) and (d) with $\widetilde{V}_0=1.9$, (e) and (f) with $\widetilde{V}_0=1.975$, and (g) and (h) with $\widetilde{V}_0=2$. The attracting procession from transient chaos to the corresponding final state takes about $t'=0.06$ s for $x=0$, that is, $\zeta_{x=0}=kv_Lt'\approx 2000$, and any transient state is plotted from $\zeta=0$ to $\zeta=100$. The left column describes the transient chaotic attractors and the right column denotes the final regular attractors and a stationary chaotic state (h).

In Fig. 2 we show that transient chaotic attractors are formed from $\zeta=0$ to $\zeta=100$. For different value of $\widetilde{V}_0$, the chaotic attractor is changed into different regular attractors with the increase of the space-time coordinate from $\zeta=100$ to $\zeta=2000$. When $\widetilde{V}_0=1.85$ is taken, Fig. 2(b) shows the final attractor as a closed single-period orbit. As the optical intensities are increased to $\widetilde{V}_0=1.9$ and $\widetilde{V}_0=1.975$, the final phase orbits become the double-period and four-period orbits as in Figs. 2(d) and 2(f). When the laser strength reaches $\widetilde{V}_0=2$ by carefully adjusting our numerical simulations, the phase trajectories fall from the transient chaotic state as in Fig. 2(g) onto the stationary chaotic attractor Fig. 2(h). These processions imply that the transition from transient chaos to stationary chaos may undergo a series of bifurcations.

In order to illustrate clearly the bifurcation sequence of the final attractors, we give a bifurcation plot for the value of $R(T)$ versus $\widetilde{V}_0$ as in Fig. 3, by using the same system parameters as in Fig. 2 and a different damping $\gamma=0.25$. Here, $R(T)$ is the value at $\zeta=T=n\pi$ with n being an integral number. In order to avoid transient chaos, the values of $R(T)$ in the initial 500 periods of the driven potential $V(\zeta)$ are eliminated.

From Fig. 3 we can see that for small $\widetilde{V}_0$ the evolutional behavior of the system converges to a period-1 solution. With increase of the optical intensity the first bifurcation appears at about $\widetilde{V}_0=2.82$, and the second bifurcation at about $\widetilde{V}_0=2.92$. As expected, the transition between transient chaos and stationary chaos indeed comes through a period-doubling bifurcation. Comparing Fig. 2 with Fig. 3, we find that for a larger damping 0.25 in Fig. 3 the critical optical strength $\widetilde{V}_0$ for the stationary chaos also becomes stronger.

For the sake of seeking the effect of damping on the onset of chaos in this system, we plot the bifurcation graphic of $R(T)$ versus the damping γ as in Fig. 4, where the system parameters are the same as in Fig. 2 and the optical potential strength is taken as a determined number $\widetilde{V}_0=1.8$. From Fig. 4 we can see that for much weaker damping the values of $R(T)$ are random and the motion of the system is stationary chaotic. When the damping becomes stronger, the values of $R(T)$ convergence to two values and the motion of the system becomes regular. Thereby, the damping plays a baffling role in obstructing the system coming into stationary chaos. This result is in agreement with the theoretical analysis in the above-mentioned Melnikov method.

Going back over the above theoretical analysis and numerical simulation, the evolution of the matter wave is governed by a Bloch-like wave in Eq. (2), which is traveling with the same velocity as the optical lattice. Therefore, the random motions in the deterministic system demonstrate to us a time-space chaos. This chaotic state propagates in the direction of motion of the optical lattice.

IV. CONCLUSION

In summary, we have considered a BEC system loaded into a moving lattice and studied the space-time chaotic dynamics of the system. When the optical lattice potential and the damping are very weak, using the Melnikov function to predict the onset of chaos is a valid analytical technique. In the perturbational parameter region, the Melnikov chaos near the homoclinic solution was investigated for the evolution of the atomic number density, and the weak chaotic regime was presented consequently. A chaos suppression effect caused by the propagation of the optical lattice was revealed, which suggests a possible method for controlling chaos in experiments. When the intensity of the optical lattice potential and the damping are strong enough, the Melnikov method becomes invalid, which necessitates a numerical approach. A chaotic transient, which is a common phenomenon in dissipative systems, has been illustrated numerically. The transition from the transient to stationary chaos was embodied in the variety of the final attractors. The route from transient

chaos to a stationary chaotic state of the system was simulated numerically and period-doubling bifurcations were demonstrated when the strength of the lattice potential was increased continuously. Meanwhile, the restraining effects on the onset of chaos caused by the damping were also investigated.

In the recent advancements in applications of BECs, quantum computation with BEC atoms in Mott insulating states is an interesting subject [18]. However, chaos is associated with quantum entanglement [47] and quantum error correcting [48], which are all key subjects in quantum computation; thereby, investigating and controlling the chaos in BECs is very important.

ACKNOWLEDGMENT

This work was supported by the National Natural Science Foundation of China under Grant No. 10275023.

[1] J. P. Dowling and J. Gea-Banacloche, Adv. At., Mol., Opt. Phys. **37**, 1 (1996).
[2] R. Grimm, M. Weidemüller, and Yu. B. Ovchinnikov, Adv. At., Mol., Opt. Phys. **42**, 95 (2000).
[3] S. Bernet, R. Abfalterer, C. Keller, M. K. Oberthaler, J. Schmiedmayer, and A. Zeilinger, Phys. Rev. A **62**, 023606 (2000).
[4] B. P. Anderson and M. A. Kasevich, Science **282**, 1686 (1998).
[5] M. Greiner, O. Mandel, T. Esslinger, T. W. Hänsch, and I. Bloch, Nature (London) **415**, 39 (2002).
[6] H. Xiong, S. Liu, and G. Huang, J. Phys. B **36**, L121 (2003).
[7] J. C. Bronski, L. D. Carr, B. Deconinck, and J. N. Kutz, Phys. Rev. Lett. **86**, 1402 (2001); J. C. Bronski, L. D. Carr, B. Deconinck, J. N. Kutz, and K. Promislow, Phys. Rev. E **63**, 036612 (2001).
[8] D. I. Choi and Q. Niu, Phys. Rev. Lett. **82**, 2022 (1999).
[9] C. Orzel, A. K. Tuchman, M. L. Fenselau, M. Yasuda, and M. A. Kasevich, Science **291**, 2386 (2001).
[10] B. Wu and Q. Niu, Phys. Rev. A **64**, 061603(R) (2001).
[11] M.-O. Mewes *et al.*, Phys. Rev. Lett. **78**, 582 (1997).
[12] F. S. Cataliotti, S. Burger, C. Fort, P. Maddaloni, F. Minardi, A. Trombettoni, A. Smerzi, and M. Inguscio, Science **293**, 843 (2001).
[13] L.-M. Duan, E. Demler, and M. D. Lukin, Phys. Rev. Lett. **91**, 090402 (2003).
[14] S. Liu, H. Xiong, Z. Xu, and G. Huang, J. Phys. B **36**, 2083 (2003).
[15] S. Burger *et al.*, Phys. Rev. Lett. **86**, 4447 (2001).
[16] W. Hai, G. Chong, Q. Xie, and J. Lu, Eur. Phys. J. D **28**, 267 (2004); W. Hai, C. Lee, X. Fang, and K. Gao, Physica A **335**, 445 (2004).
[17] K. Burnett, M. Edwards, C. W. Clark, and M. Shotter, J. Phys. B **35**, 1671 (2002).
[18] J. K. Pachos and P. L. Knight, Phys. Rev. Lett. **91**, 107902 (2003).
[19] R. Ionicioiu and P. Zanardi, Phys. Rev. A **66**, 050301(R) (2002).
[20] D. V. Strekalov, A. Turlapov, A. Kumarakrishnan, and Tycho Sleator, Phys. Rev. A **66**, 023601 (2002).
[21] D. van Oosten, P. van der Straten, and H. T. C. Stoof, Phys. Rev. A **63**, 053601 (2001).
[22] M. P. A. Fisher *et al.*, Phys. Rev. B **40**, 546 (1989).
[23] A. Smerzi, S. Fantoni, S. Giovanazzi, and S. R. Shenoy, Phys. Rev. Lett. **79**, 4950 (1997).
[24] C. Lee, W. Hai, L. Shi, X. Zhu, and K. Gao, Phys. Rev. A **64**, 053604 (2001).
[25] W. Hai, C. Lee, G. Chong, and L. Shi, Phys. Rev. E **66**, 026202 (2002); Q. Xie, W. Hai, and G. Chong, Chaos **13**, 801 (2003); G. Chong, W. Hai, and Q. Xie, *ibid.* **14**, 217 (2004).
[26] R. Franzosi and V. Penna, Phys. Rev. E **67**, 046227 (2003).
[27] Q. Thommen, J. C. Garreau, and V. Zehnlé, Phys. Rev. Lett. **91**, 210405 (2003).
[28] P. A. Ruprecht, M. Edwards, K. Burnett, and C. W. Clark, Phys. Rev. A **54**, 4178 (1996).
[29] P. Öhberg and S. Stenholm, J. Phys. B **32**, 1959 (1999).
[30] J. H. Denschlag *et al.*, J. Phys. B **35**, 3095 (2002).
[31] L. Fallani, F. S. Cataliotti, J. Catani, C. Fort, M. Modugno, M. Zawada, and M. Inguscio, Phys. Rev. Lett. **91**, 240405 (2003).
[32] V. S. Filho, A. Gammal, T. Frederico, and L. Tomio, Phys. Rev. A **62**, 033605 (2000).
[33] H. Saito and M. Ueda, Phys. Rev. Lett. **86**, 1406 (2001).
[34] F. Dalfovo, S. Giorgini, L. P. Pitaevskii, and S. Stringari, Rev. Mod. Phys. **71**, 463 (1999).
[35] V. K. Melnikov, Trans. Mosc. Math. Soc., **12**, 1 (1963).
[36] J.-P. Eckmann and D. Ruelle, Rev. Mod. Phys. **57**, 617 (1985).
[37] J. Hoffnagle and R. G. Brewer, Science **265**, 213 (1994); Phys. Rev. Lett. **71**, 1828 (1993); Phys. Rev. A **50**, 4157 (1994).
[38] Jing-Ling Shen, Hua-Wei Yin, Jian-Hua Dai, and Hong-Jun Zhang, Phys. Rev. A **55**, 2159 (1997).
[39] I. Zapata, F. Sols, and A. J. Leggett, Phys. Rev. A **57**, R28 (1998).
[40] I. Marino, S. Raghavan, S. Fantoni, S. R. Shenoy, and A. Smerzi, Phys. Rev. A **60**, 487 (1999).
[41] F. Kh. Abdullaev and R. A. Kraenkel, Phys. Rev. A **62**, 023613 (2000).
[42] A. Aftalion, Q. Du, and Y. Pomeau, Phys. Rev. Lett. **91**, 090407 (2003).
[43] A. H. Nayfeh and D. T. Mook, *Nonlinear Oscillatons* (Wiley, New York, 1979).
[44] Z. Liu, *Perturbation Criteria for Chaos* (Shanghai Scientific and Technological Education Press, Shanghai, 1994) (in Chinese).
[45] A. Venkatesan, M. Lakshmanan, A. Prasad, and R. Ramaswamy, Phys. Rev. E **61**, 3641 (2000).
[46] W. L. Ditto *et al.*, Phys. Rev. Lett. **63**, 923 (1989); H. T. Savage *et al.*, J. Appl. Phys. **67**, 5619 (1990).
[47] K. Furuya, M. C. Nemes, and G. Q. Pellegrino, Phys. Rev. Lett. **80**, 5524 (1998).
[48] P. H. Song and D. L. Shepelyansky, Phys. Rev. Lett. **86**, 2162 (2001).